RSC Advances

View Online
Dynamic Article Links

Cite this: *RSC Advances*, 2011, **1**, 917–922

www.rsc.org/advances

PAPER

Insight into the crystal synthesis, activation and application of ZIF-20†

Beatriz Seoane,[a] Juan M. Zamaro,[b] Carlos Téllez[a] and Joaquín Coronas*[a]

Received 10th May 2011, Accepted 30th June 2011
DOI: 10.1039/c1ra00164g

The crystallization of the zeolitic imidazolate framework ZIF-20 has been tuned from the point of view of crystal size and aggregation by using rotation and seeding with a previously prepared material. In addition, the activation of ZIF-20 by solvent extraction has been found to be in correlation with the relative permittivity of the solvent. High permittivity solvents (acetone and methanol) extract more guest dimethylformamide but amorphize the structure, while those with low permittivity (n-pentane and chloroform) preserve the crystallinity of ZIF-20. The dispersion in commercial polysulfone of the small synthesized ZIF-20 particles obtained with low aggregation results in an improved O_2-selective mixed matrix membrane (O_2 permeability and O_2/N_2 selectivity being 1.0 ($\pm$0.0) Barrer and 6.7 ($\pm$0.5), respectively).

1. Introduction

Metal Organic Frameworks (MOFs) are crystalline tridimensional networks consisting of metal ions or metal clusters bridged by organic linkers.[1,2] They are characterized by high specific surface area and pore volume. They are highly versatile materials in the sense that by choosing the appropriate organic ligand it is possible to determine the size, shape and chemical functionality of their cavities.[3–6] For these reasons, MOFs have a great potential for application in gas storage,[2,7,8] drug delivery,[9] gas separation with membranes,[10,11] enantioselective separations,[12] sensors,[13] and heterogeneous catalysis.[14,15]

Zeolitic imidazolate frameworks (ZIFs) are a subclass of MOFs that have similar topologies to those of zeolites and possess a chemical and thermal stability higher than other types of MOFs.[16–19] They consist of transition metals, generally divalent, such as Cu (II), Zn (II), Co (II), Cd (II), *etc.* linked in tetrahedral coordination through imidazole derivatives (methylimidazole, benzylimidazole, purine, *etc.*). They form an electrically neutral three-dimensional network.[20] In particular, ZIF-20 has a pore opening of 2.8 Å, a Langmuir specific surface area of 800 m^2/g (measured with Ar) and a pore volume of 0.27 cm^3/g.[18] Its isotropic 3D channel network with small openings and bulky cavities means that it does not require the development of membranes with preferential crystallographic orientation, making this material especially suitable for the separation of small molecules. In addition, the partially organic nature of ZIF-20 must provide a better interaction with a polymer phase in a mixed matrix membrane (MMM).[21] Despite these advantages, there is the common problem in MOFs that after synthesis the solvent molecules trapped in the pores of the material must be evacuated (activation) to create the permanent porosity in the solid. Different activation procedures may originate different textural properties for the same material,[22] and in many cases the evacuation of MOFs is not achieved without a degradation of the crystal structure. For example, from a series of 10 Co- and Zn-based ZIFs with good thermal stability only one structure maintained its integrity after activation.[23]

On the other hand, the use of microporous materials for gas separation can be accomplished through MMMs which consist of a continuous polymeric phase that disperses particles of the microporous material. Two critical aspects in the preparation of MMMs are the morphological characteristics of crystals and their chemical compatibility with the polymer phase. To maximize the adhesion between both phases, it is preferable to use non-aggregated particles of a few micrometers in size and with a similar hydrophobicity to that of the polymer.[24] Recently, MMMs containing MOFs have been obtained as CuTPA/Poly(vinyl acetate),[25] Cu-4,4′-bypiridine-hexafluorosilicate (Cu-BPY-HFS)/polyimide,[26] MOF-5/polyimide,[27] and $Cu_3(BTC)_2$/ polyimide.[28] These membranes showed good permeability properties for pure gases, such as He, CO_2, O_2, N_2, and CH_4, and good separation performance of binary mixtures, such as CO_2/CH_4, H_2/CO_2, and CH_4/N_2. Membranes containing ZIFs have been also reported: ZIF-8/1,4-phenylene ether-ether-sulfone,[29] ZIF-8/polyimide,[30] and ZIF-90/polyimide[11] that were applied to the separation of H_2/CO_2 and CO_2/CH_4 gas mixtures.

In this work, the synthesis of ZIF-20 has been studied to reduce the crystal particle size and level of aggregation. Different activation procedures were carried out trying to preserve the crystallinity of ZIF-20. Finally, ZIF-20/polysulfone membranes were prepared and evaluated in O_2/N_2 separation.

2. Experimental

2.1. Synthesis of ZIF-20

The basic synthesis of the ZIF-20 material was performed in accordance with ref. 18 employing a solution with a Zn

[a]*Chemical and Environmental Engineering Department and Instituto de Nanociencia de Aragón (INA), Universidad de Zaragoza, Zaragoza, 50018, Spain. E-mail: coronas@unizar.es.*
[b]*Instituto de Investigaciones en Catálisis y Petroquímica, INCAPE (FIQ, UNL, CONICET), Santiago del Estero 2829, 3000 Santa Fe, Argentina*
† Electronic supplementary information (ESI) available. See DOI: 10.1039/c1ra00164g

concentration of 0.05 mol/L and a Zn/organic linker ratio of 0.2. In a typical synthesis $Zn(NO_3)_2{\cdot}6H_2O$ (74 mg, 0.25 mmol, Sigma-Aldrich) and purine (150 mg, 1.25 mmol, Sigma-Aldrich) were dissolved in 5 mL of dimethylformamide (DMF) (Alfa Aesar) inside a 45 mL stainless steel Teflon-lined autoclave. After 30 min of stirring the autoclave was capped and then heated at 65 °C in an air convection oven.

The synthesis of ZIF-20 was studied by varying the crystallization time (24, 48, and 72 h), while several solvothermal treatments were performed under static and rotation conditions (30 r.p.m.) and with seeding (0.4 and 1.2 wt % of seeds with respect to the total amount of ZIF-20 product recovered).

The activation of the materials was carried out by solvent exchange in a number of solvents (n-pentane, chloroform, acetone, methanol, and water) with and without stirring for different exchanging times (36, 24 and 72 h) and at room temperature. In a typical procedure, ZIF-20 powder (40 mg) was immersed in the solvent (4 mL) which was refreshed every 12 h. Finally, the samples were evacuated at 70 °C for 10 h under vacuum conditions to obtain activated crystals.

2.2. Preparation of ZIF-20 MMMs

Polysulfone (PSF) Udel® P-3500 (kindly supplied by Solvay Advanced Polymers) was used as the continuous phase for the MMMs. This amorphous, high performance polymer presents good solubility in many solvents such as dichloromethane, chloroform or tetrahydrofurane and shows excellent mechanical and thermal properties with a glass transition temperature of 188 °C.

Before fabricating the membranes, PSF was dried under vacuum conditions at 120 °C for 24 h. First, bare PSF membranes were prepared to compare their results with those of membranes containing 8 wt% ZIF-20 crystals as the dispersed phase. These MOF–free membranes were obtained by dissolving the polymer (0.4 g) in chloroform (3.6 g, Sigma-Aldrich) and stirring overnight. The percentage of the solvent was 90 wt% and was selected to assure a good viscosity of the casting solution. The preparation of the ZIF-20/PSF membranes was identical but with an additional step for dispersing the ZIF-20 particles in the solvent in an ultrasonic bath for 15 min. The polymer was then added and the dispersion obtained was stirred overnight. Subsequently, the membranes were cast on flat glass plates, and left partially closed to slow down the natural evaporation of solvent under ambient conditions. The final step consisted of removing the remaining solvent under vacuum conditions at 120 °C for 24 h.

The membranes obtained had a thickness of around 75–100 μm, measured using a Digimatic Micrometer (Mitutoyo Quickmike Series 293-IP-54 Absolute 0–30 mm with an accuracy of ± 0.001 mm).

2.3. Characterization

The formation of ZIF-20 phase was confirmed by X-ray diffraction. The studies were performed at ambient temperature on a rotating anode diffractometer (D-Max Rigaku) using monochromatic CuKα radiation with λ = 1.5418 Å with a scanning rate of 0.03°/s between 2θ = 2.5° and 40°. Scanning electron microscopy (SEM) images of the ZIF-20 particles and the MMMs fabricated were acquired with a JEOL JSM 6400 SEM instrument operating at 20 kV. For this purpose, cross sectional pieces of the membrane were prepared by freeze fracturing after immersion in liquid N_2. All samples were coated with a thin film of Au. The removal of the guest molecules from the pores of ZIF-20 crystals was studied by means of thermogravimetric analysis. The analyses were performed under N_2 atmosphere from 25 to 800 °C with a heating rate of 5 °C/min using a Mettler Toledo TGA/SDTA851e system. The pore volume was calculated by applying the Dubinin–Radushkevitch equation. The adsorbate used was CO_2 and the measurements were run at 25 °C with a Micromeritics ASAP 2020 V1.04 H after outgassing the sample at 70 °C for 10 h. FTIR spectra of ZIF-20 (5 mg)-KBr pills were recorded with a Shimadzu IRAffinity instrument in the wavenumber range 400–4000 cm^{-1}.

A detailed description of the gas permeation setup is reported elsewhere.[31] The membranes with an area of 15.2 cm^2 were placed inside a permeability module composed of two stainless steels parts with a cavity in one of them in which a macroporous stainless steel disk (Mott, 20 μm nominal pore size) was placed as support. Mass flow meter controllers (Alicat Scientific) were used for feed and sweep gas provision to the membrane module. A O_2/N_2 (25/25 cm^3(STP)/min) mixture stream was fed at 45 psia to the retentate side, while the permeate side was swept with a He (5 cm^3(STP)/min) stream at 18 psia. The gas concentrations in the outgoing stream were analyzed by an on-line gas micro-chromatograph Agilent 3000A equipped with TCD. The permeability was calculated in Barrer (1 Barrer= 1×10^{-10} cm^3 (STP)·cm/(cm^2·s·cmHg)) and the selectivity was established as the ratio of permeabilities. All the measurements were performed at 35 °C.

3. Results and discussion

3.1. Crystal and aggregate size control of ZIF-20

ZIF-20[18] is the topological analogue of the LTA-type zeolite (Fig. 1a). It is composed of Zn (II) atoms linked by purine molecules *via* the N atoms of the imidazole ring (Fig. 1b).

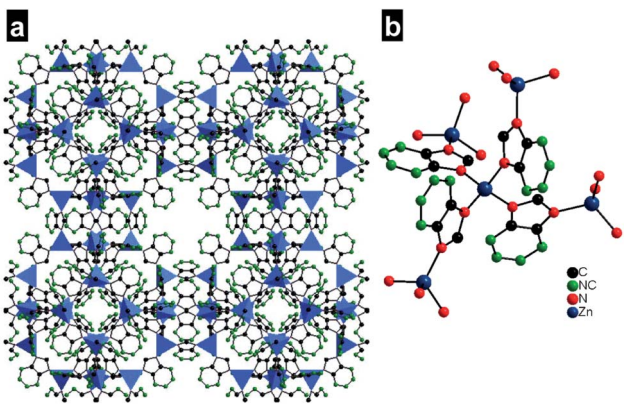

Fig. 1 Diagram of ZIF-20 showing: (a) the crystal structure with the LTA topology as zeolite A, and (b) the local coordination environment and connectivity between inorganic and organic components (NC corresponds to N=C double bonds). Structures were built using Diamond software with CCDC archive for ZIF-20.

A variable that has been demonstrated to have an influence on the crystal size of several materials including zeolites is the agitation of the synthesis mixture during the hydrothermal treatment. Dynamic conditions can accelerate the nucleation rate and then produce smaller crystals. Following this criterion, solvothermal synthesis with rotation of the media was carried out. Fig. 2 shows the XRD pattern of ZIF-20 powder obtained at the same temperature as that reported by Hayashi *et al.*[18] (65 °C) in static conditions and those obtained under rotation and synthesis times of 1, 2, and 3 days. It can be seen that in static conditions a pure phase of ZIF-20 was obtained consistent with the reported intensities for this structure. The dynamic synthesis results indicate that 2 days are necessary to obtain the high crystalline phase. Moreover, it was observed that the particle size of crystalline materials can be tuned by controlling the synthesis conditions. Fig. 3 depicts the SEM images corresponding to the samples that were analyzed by XRD. As shown in Fig. 3 and Table 1, it can be observed that crystal and aggregate sizes were considerably reduced from the static synthesis conditions (10.9 ± 8.4 μm and 190 ± 146 μm, respectively) to the 2 days rotation synthesis which gave rise to the smallest and less agglomerated crystals (3.6 ± 0.8 μm and 10.4 ± 2.6 μm, respectively). The crystals obtained under rotation conditions have a relatively small and uniform size which can favor the interaction with the polymeric phase in a MMM.

As Fig. 2 shows, the seeding allowed the preparation of high crystalline ZIF-20 even after 1 day of rotating synthesis. From the point of view of small particle size and minimum agglomeration, the best results with seeding were obtained from the smallest amount of seeds used (0.4 wt%) (see Fig. 4 and Table 1) giving rise to crystal and aggregate sizes of 4.2 ± 1.5 μm and 15.3 ± 5.9 μm, respectively. All average crystal and aggregate sizes with their errors for the studied samples are presented in Table 1.

3.2. Activation of ZIF-20

Analogously to zeolites synthesized using organic structure directing agents (OSDA), solvent molecules used during the solvothermal synthesis of ZIFs (and MOFs in general) act as templates filling the microporosity. While in zeolites OSDAs are removed by calcination at 500–800 °C depending on the corresponding pore size,[32] the solvent molecules trapped in MOFs are commonly evacuated through direct thermal treatment of the solids in N_2 or vacuum atmosphere[16,33] or performing previous exchange with more volatile solvents (*i.e.* methanol, chloroform) that facilitates the subsequent evacuation process. This stage is carried out by heating at around the boiling temperature of the pure solvent in vacuum. This means moderate temperatures because of the limited thermal stabilities of MOFs.[22] The reported activation treatment for ZIF-20 involved a methanol exchange and vacuum evacuation.[18]

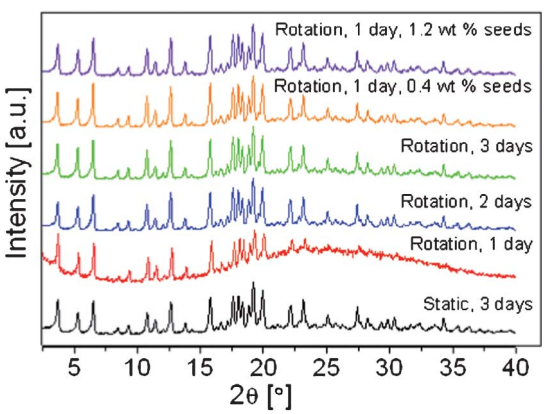

Fig. 2 XRD patterns of ZIF-20 powders obtained under static and rotation conditions for 1, 2, and 3 days and for 1 day with 0.4 and 1.2 wt% seeding.

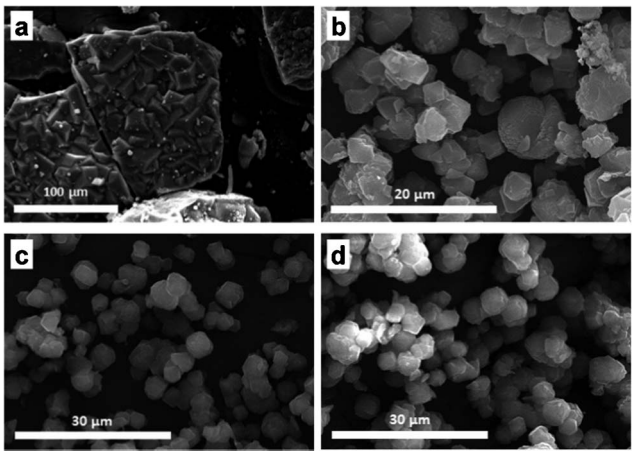

Fig. 3 SEM images of ZIF-20: (a) material obtained following the report from Hayashi *et al.*[18] (static, 3 days at 65 °C); (b–d) materials obtained at the same temperature in rotation conditions after 1, 2, and 3 days of synthesis, respectively.

The activation (and simultaneously the chemical stability) of ZIF-20 has been studied in n-pentane, chloroform, acetone, methanol, and water for 1 and 3 days at room temperature. Fig. 5 shows that after 1 day the material remains stable in n-pentane, chloroform and acetone but sample in methanol shows an important increase in the XRD base line indicating amorphization. For sample kept in water, the ZIF-20 structure clearly transforms into an unknown and denser phase (since the lowest 2θ value is now about 9°). Fig. 6 shows the XRD patterns of samples after 3 days in contact with the solvents: only n-pentane and chloroform leave the crystallinity of ZIF-20 unaltered.

Permittivity relates to the ability of a certain material to transmit an electric field and in the case of solvents gives an idea of their polarity. The higher the value of permittivity is, the more polar the solvent. Fig. 7 shows the DMF remaining in the solids

Table 1 Crystal and aggregate sizes of ZIF-20 synthesized in different conditions

Synthesis conditions	Crystals [μm]	Aggregates [μm]
Static, 3 d	10.9 (±8.4)	190 (±146)
Rotation, 1 d	4.0 (±1.1)	17.6 (±5.3)
Rotation, 2 d	3.6 (±0.8)	10.4 (±2.6)
Rotation, 3 d	3.8 (±0.9)	14.9 (±4.9)
Rotation, 1 d, 0.4 wt % seeds	4.2 (±1.5)	15.3 (±5.9)
Rotation, 1 d, 1.2 wt % seeds	1.9 (±0.3)	36.6 (±10.1)

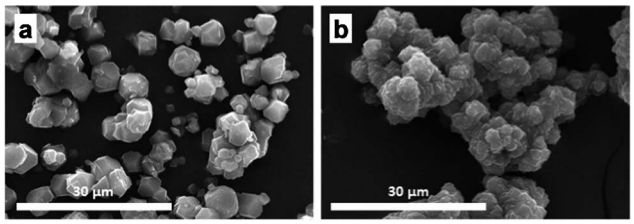

Fig. 4 SEM images of ZIF-20 obtained under rotation conditions for 1 day with 0.4 (a), and 1.2 (b) wt% seeding.

as determined by TGA of samples corresponding to Fig. 5 and 6. Note that the four solvents are much more volatile compounds (boiling points: 36, 61, 56, and 65 °C for n-pentane, chloroform, acetone, and methanol, respectively) than DMF (boiling point: 153 °C); in consequence, the assignation of weight loss to DMF in the 100–250 °C range of temperature is unambiguous (see Fig. S1, ESI)†. The amount of DMF trapped in ZIF-20 after exchange decreases as a function of the relative permittivity of the solvent, indicating a preferential exchange of DMF by polar solvents. However, acetone and methanol amorphize the ZIF-20 structure as discussed above. The amorphization observed with high polarity solvents could be due to their strong interaction with polar centers in the framework giving rise to the collapse of the material. Hence, chloroform was chosen as the better solvent for exchange in more efficient conditions (under stirring and 36 h), giving rise to minimum remains of DMF (2.5 wt % *vs.* 15.4 wt % in the as-made material) in ZIF-20 (Fig. S1† and Fig. 7). The evacuation was also followed by FTIR analysis of the materials (Fig. S2)†. The best sample, exchanged with chloroform under stirring conditions and evacuated under vacuum at 70 °C for 10 h, was submitted to CO_2 adsorption measurements (Fig. S3)† obtaining a Dubinin–Radushkevitch pore volume of 0.20 ($\pm$0.00) cm^3/g, in good agreement with that previously reported for the same material.[18] Finally, it is worth mentioning that direct thermal activation in N_2 (at 200 °C with 0.1 °C/min heating rate), without the solvent exchange step, produced the total loss of crystallinity (as seen by XRD).

3.3 ZIF-20/PSF MMM

The performance of ZIF-20 obtained under rotation conditions for 2 days (lowest agglomeration with crystal size below 4 μm) was tested as filler on MMMs for O_2/N_2 separation (Table 2). Several membranes were prepared by dispersing 8 wt% of ZIF-20 in commercial polysulfone Udel®. Note that the solvent used for the MMM preparation was that giving rise to the best solvent extraction achievement, so that the compatibility between the crystal synthesis (crystallization and activation) and membrane preparation was total. The O_2/N_2 membrane separation corresponds to the most extensively investigated gas pair, while the 8 wt% filler loading was selected because it has been shown to produce maximum selectivity increases with certain zeolitic fillers.[34,35] The cross-section SEM image in Fig. 8 reveals a homogeneous dispersion and an intimate contact between both the metal–organic and continuous organic media, discarding by-pass transport through interphases. The interaction between the filler and the matrix is improved by the expected affinity between the organic part of ZIF-20 and the polymer. In the XRD diffraction pattern of Fig. 9 it can be seen that, in spite of the high intensity amorphous signal coming from the polymer phase, some of the main ZIF-20 reflection peaks are present in the composite membrane. In addition, the broad peak for the pure polymer centered at 2θ = 17.3° (d-spacing= 5.1 Å) moves to 17.9° (d-spacing= 5.0 Å), in agreement with a strong interaction

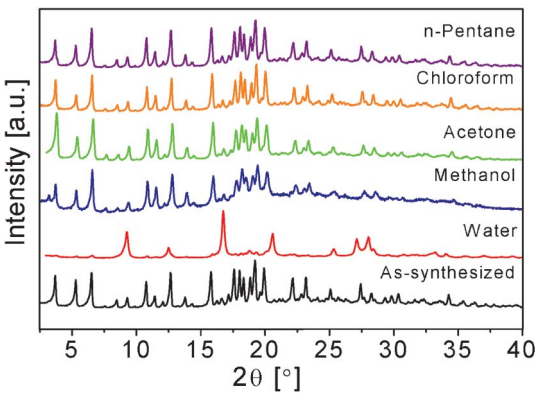

Fig. 5 XRD patterns of ZIF-20 powders after contacting with different solvents at room temperature for 1 day.

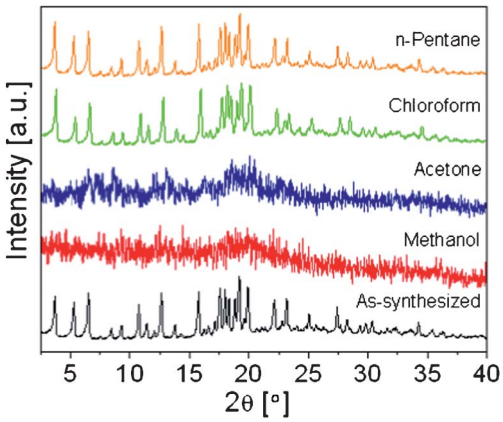

Fig. 6 XRD patterns of ZIF-20 powders after contacting with different solvents at room temperature for 3 days.

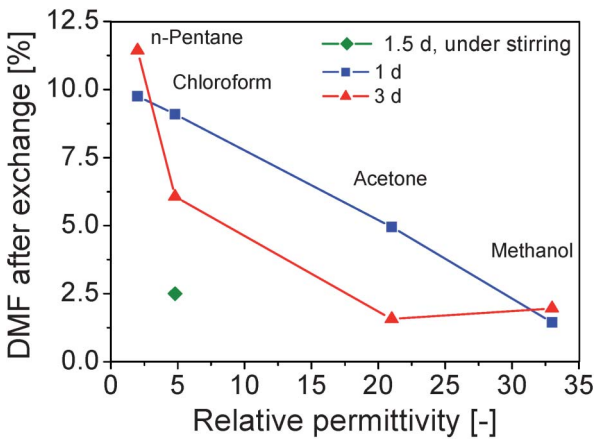

Fig. 7 Remaining DMF (as determined by TGA) after solvent exchange as a function of solvent relative permittivity.

Table 2 Performance of the 8 wt% ZIF-20/PSF MMM in the separation of a O_2/N_2 mixture at 35 °C[a]

Membrane	Permeability [Barrer]		O_2/N_2 Selectivity
	O_2	N_2	
Pure PSF	1.6 (±0.2)	0.34 (±0.05)	4.7 (±0.4)
8 wt % ZIF-20/PSF	1.0 (±0.0)	0.15 (±0.01)	6.7 (±0.5)

[a] Four membranes were tested to calculate average and standard deviation values. Pure PSF values were taken from a previous report using the same experimental set up and conditions.[34]

between continuous and disperse phases which would reduce the distance between polymer chains.[34]

Concerning the gas separation, while the O_2 permeability showed a small decrease from 1.6 (±0.2) for pure PSF to 1.0 (±0.0) Barrer for the MMM, the O_2/N_2 selectivity increased from 4.7 (±0.4) to 6.7 (±0.5) as shown in Table 2. The relatively small difference in kinetic size between O_2 (kinetic diameter d_k= 0.343 nm) and N_2 (d_k= 0.368 nm) would justify the increasing sieving effect observed in the MMM. In fact, it has been reported that it is difficult to characterize ZIF-20 by N_2 adsorption because of its slow diffusion, so that Ar (d_k= 0.342 nm) has been used as adsorbate giving rise to the measurement of 800 m^2/g of Langmuir area.[18] Finally, obtaining a volume fraction of 0.091 from the weight filler loading and PSF (1.24 g/cm^3) and ZIF-20 (1.04 g/cm^3)[36] densities and using the so-called Reduced Mobility Modified Maxwell Model[37] (interphase thickness = 1.4 μm, chain immobilization factor = 5.2), it has been estimated an O_2 permeability of 45 Barrer through the ZIF-20 filler dispersed in PSF. This permeability agrees with that obtained through a ZIF-7 pure membrane[38] for single gases like CO_2, N_2 or CH_4, ZIF-20 (0.28 nm) having a pore size similar to that of ZIF-7 (0.29 nm).

Conclusions

The use of rotation and seeding allowed the diminishing of both crystal and agglomerate sizes of ZIF-20 with respect to the published synthesis conditions. A direct correlation has been found between solvent relative permittivity and the solvent exchange: the higher the permittivity of the solvent (acetone and methanol), the more efficient the removal of DMF from the as-made material. However, low permittivity solvents (n-pentane and chloroform) preserve the crystallinity of ZIF-20, something that was not achieved under 1–3 days contact with acetone or methanol. Once it was concluded that chloroform preserves the crystallinity of ZIF-20, more efficient conditions were applied to exchange most of the DMF in the material (as demonstrated by TGA and FTIR).

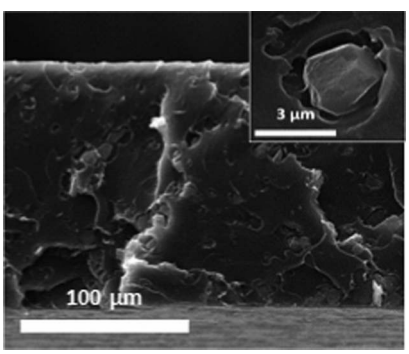

Fig. 8 SEM image of 8 wt% ZIF-20/PSF MMM.

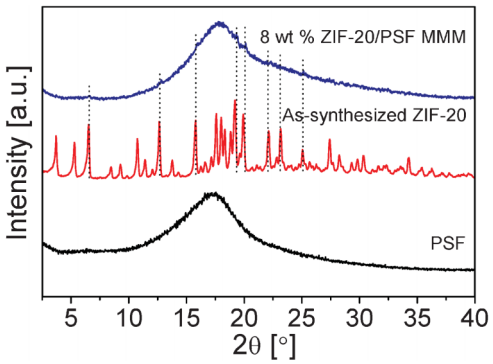

Fig. 9 XRD patterns of pure PSF, as-synthesized ZIF-20, and 8 wt% ZIF-20/PSF MMM.

As a first attempt to exploit the suitability of the small and less agglomerated ZIF-20 crystals prepared, 8 wt% ZIF-20/polysulfone mixed matrix membranes have been shown to give a better performance in the separation of an equimolar O_2/N_2 mixture than the pure polymer.

Acknowledgements

Financial support (CIT-420000-2009-32, MAT2010-15870) and a FPU Program fellowship (B. Seoane) from the Spanish Science and Innovation Ministry are gratefully acknowledged. J. M. Zamaro acknowledges CONICET of Argentina for a grant for a research stay in Spain.

References

1 O. M. Yaghi, M. O'Keeffe, N. W. Ockwig, H. K. Chae, M. Eddaoudi and J. Kim, *Nature*, 2003, **423**, 705–714.
2 G. Ferey, *Chem. Soc. Rev.*, 2008, **37**, 191–214.
3 M. Eddaoudi, J. Kim, N. Rosi, D. Vodak, J. Wachter, M. O'Keeffe and O. M. Yaghi, *Science*, 2002, **295**, 469–472.
4 S. Kitagawa, R. Kitaura and S. Noro, *Angew. Chem., Int. Ed.*, 2004, **43**, 2334–2375.
5 H. K. Chae, D. Y. Siberio-Perez, J. Kim, Y. Go, M. Eddaoudi, A. J. Matzger, M. O'Keeffe and O. M. Yaghi, *Nature*, 2004, **427**, 523–527.
6 S. L. Qiu and G. S. Zhu, *Coord. Chem. Rev.*, 2009, **253**, 2891–2911.
7 J. L. C. Rowsell and O. M. Yaghi, *Angew. Chem., Int. Ed.*, 2005, **44**, 4670–4679.
8 U. Mueller, M. Schubert, F. Teich, H. Puetter, K. Schierle-Arndt and J. Pastre, *J. Mater. Chem.*, 2006, **16**, 626–636.
9 P. Horcajada, C. Serre, M. Vallet-Regi, M. Sebban, F. Taulelle and G. Ferey, *Angew. Chem., Int. Ed.*, 2006, **45**, 5974–5978.
10 H. Bux, F. Y. Liang, Y. S. Li, J. Cravillon, M. Wiebcke and J. Caro, *J. Am. Chem. Soc.*, 2009, **131**, 16000–16001.
11 T. H. Bae, J. S. Lee, W. L. Qiu, W. J. Koros, C. W. Jones and S. Nair, *Angew. Chem., Int. Ed.*, 2010, **49**, 9863–9866.
12 J. S. Seo, D. Whang, H. Lee, S. I. Jun, J. Oh, Y. J. Jeon and K. Kim, *Nature*, 2000, **404**, 982–986.
13 Y. Takashima, V. M. Martinez, S. Furukawa, M. Kondo, S. Shimomura, H. Uehara, M. Nakahama, K. Sugimoto and S. Kitagawa, *Nat. Commun.*, 2011, **2**, 8.
14 S. Naito, T. Tanibe, E. Saito, T. Miyao and W. Mori, *Chem. Lett.*, 2001, 1178–1179.
15 T. Sato, W. Mori, C. N. Kato, E. Yanaoka, T. Kuribayashi, R. Ohtera and Y. Shiraishi, *J. Catal.*, 2005, **232**, 186–198.
16 K. S. Park, Z. Ni, A. P. Cote, J. Y. Choi, R. D. Huang, F. J. Uribe-Romo, H. K. Chae, M. O'Keeffe and O. M. Yaghi, *Proc. Natl. Acad. Sci. U. S. A.*, 2006, **103**, 10186–10191.

17 X. C. Huang, Y. Y. Lin, J. P. Zhang and X. M. Chen, *Angew. Chem., Int. Ed.*, 2006, **45**, 1557–1559.
18 H. Hayashi, A. P. Cote, H. Furukawa, M. O'Keeffe and O. M. Yaghi, *Nat. Mater.*, 2007, **6**, 501–506.
19 Y. Q. Tian, S. Y. Yao, D. Gu, K. H. Cui, D. W. Guo, G. Zhang, Z. X. Chen and D. Y. Zhao, *Chem.–Eur. J.*, 2010, **16**, 1137–1141.
20 A. Phan, C. J. Doonan, F. J. Uribe-Romo, C. B. Knobler, M. O'Keeffe and O. M. Yaghi, *Acc. Chem. Res.*, 2010, **43**, 58–67.
21 B. Zornoza, P. Gorgojo, C. Casado, C. Tellez and J. Coronas, *Desalin. Water Treat.*, 2011, **27**, 42–47.
22 C. M. Lu, J. Liu, K. F. Xiao and A. T. Harris, *Chem. Eng. J.*, 2010, **156**, 465–470.
23 Y. Q. Tian, Y. M. Zhao, Z. X. Chen, G. N. Zhang, L. H. Weng and D. Y. Zhao, *Chem.–Eur. J.*, 2007, **13**, 4146–4154.
24 T. S. Chung, L. Y. Jiang, Y. Li and S. Kulprathipanja, *Prog. Polym. Sci.*, 2007, **32**, 483–507.
25 R. Adams, C. Carson, J. Ward, R. Tannenbaum and W. Koros, *Microporous Mesoporous Mater.*, 2010, **131**, 13–20.
26 Y. F. Zhang, I. H. Musselman, J. P. Ferraris and K. J. Balkus, *J. Membr. Sci.*, 2008, **313**, 170–181.
27 E. V. Perez, K. J. Balkus, J. P. Ferraris and I. H. Musselman, *J. Membr. Sci.*, 2009, **328**, 165–173.
28 S. Basu, A. Cano-Odena and I. F. J. Vankelecom, *J. Membr. Sci.*, 2010, **362**, 478–487.
29 K. Diaz, L. Garrido, M. Lopez-Gonzalez, L. F. del Castillo and E. Riande, *Macromolecules*, 2010, **43**, 316–325.
30 M. J. C. Ordonez, K. J. Balkus, J. P. Ferraris and I. H. Musselman, *J. Membr. Sci.*, 2010, **361**, 28–37.
31 P. Gorgojo, S. Uriel, C. Téllez and J. Coronas, *Microporous Mesoporous Mater.*, 2008, **115**, 85–92.
32 I. Tiscornia, S. Valencia, A. Corma, C. Téllez, J. Coronas and J. Santamaría, *Microporous Mesoporous Mater.*, 2008, **110**, 303–309.
33 C. Serre, F. Millange, C. Thouvenot, M. Nogues, G. Marsolier, D. Louer and G. Ferey, *J. Am. Chem. Soc.*, 2002, **124**, 13519–13526.
34 B. Zornoza, C. Tellez and J. Coronas, *J. Membr. Sci.*, 2011, **368**, 100–109.
35 B. Zornoza, O. Esekhile, W. J. Koros, C. Tellez and J. Coronas, *Sep. Purif. Technol.*, 2011, **77**, 137–145.
36 J. C. Tan, T. D. Bennett and A. K. Cheetham, *Proc. Natl. Acad. Sci. U. S. A.*, 2010, **107**, 9938–9943.
37 T. T. Moore, T. Mahajan, D. Q. Vu and W. J. Koros, *AIChE J.*, 2004, **50**, 311–321.
38 Y. S. Li, F. Y. Liang, H. Bux, A. Feldhoff, W. S. Yang and J. Caro, *Angew. Chem., Int. Ed.*, 2010, **49**, 548–551.

